p62^{dok}, a Negative Regulator of Ras and Mitogen-activated Protein Kinase (MAPK) Activity, Opposes Leukemogenesis by p210$^{bcr\text{-}abl}$

Antonio Di Cristofano,[1] Masaru Niki,[1] Mingming Zhao,[3] Fredrick G. Karnell,[4] Bayard Clarkson,[2] Warren S. Pear,[4] Linda Van Aelst,[3] and Pier Paolo Pandolfi[1]

[1]*Department of Human Genetics, Molecular Biology Program, and* [2]*Department of Medicine, Molecular Pharmacology and Therapeutics Program, Memorial Sloan-Kettering Cancer Center, New York, NY 10021*

[3]*Cold Spring Harbor Laboratory, Cold Spring Harbor, NY 11724*

[4]*Department of Pathology and Institute for Medicine and Engineering, University of Pennsylvania, Philadelphia, PA 19104*

Abstract

p62^{dok} has been identified as a substrate of many oncogenic tyrosine kinases such as the chronic myelogenous leukemia (CML) chimeric p210$^{bcr\text{-}abl}$ oncoprotein. It is also phosphorylated upon activation of many receptors and cytoplamic tyrosine kinases. However, the biological functions of p62^{dok} in normal cell signaling as well as in p210$^{bcr\text{-}abl}$ leukemogenesis are as yet not fully understood. Here we show, in hemopoietic and nonhemopoietic cells derived from *p62$^{dok-/-}$* mice, that the loss of *p62^{dok}* results in increased cell proliferation upon growth factor treatment. Moreover, Ras and mitogen-activated protein kinase (MAPK) activation is markedly sustained in *p62$^{dok-/-}$* cells after the removal of growth factor. However, *p62^{dok}* inactivation does not affect DNA damage and growth factor deprivation–induced apoptosis. Furthermore, *p62^{dok}* inactivation causes a significant shortening in the latency of the fatal myeloproliferative disease induced by retroviral-mediated transduction of p210$^{bcr\text{-}abl}$ in bone marrow cells. These data indicate that p62^{dok} acts as a negative regulator of growth factor–induced cell proliferation, at least in part through downregulating Ras/MAPK signaling pathway, and that p62^{dok} can oppose leukemogenesis by p210$^{bcr\text{-}abl}$.

Key words: cell proliferation • signal transduction • knockout • mast cells • thymocytes

Introduction

Chronic myelogenous leukemia (CML)* is a clonal disorder of the hematopoietic cells characterized by the presence of the Philadelphia chromosome (Ph$^+$), which is the result of a chromosomal translocation between the BCR gene on chromosome 22 and the ABL gene on chromosome 9 (1). A chimeric protein known as bcr-abl originates from this translocation, and its p210 form is the causative mutation found in 95% of cases of CML. p210$^{bcr\text{-}abl}$ has heightened tyrosine kinase activity and exists exclusively in cytoplasm compared with endogenous c-ABL (2). Over an average span of 3 to 5 yr termed as chronic phase of CML, during which the Ph$^+$ cells populate the entire intermediate and late hematopoietic maturational compartments, the disease progresses leading unavoidably to an acute malignant stage known as blast crisis. The affected cells acquire additional genetic changes, and lose their ability to differentiate and mature, resulting in the functional breakdown of the hematopoietic system (3).

p62^{dok} was cloned as a major phosphorylation substrate of the p210$^{bcr\text{-}abl}$ oncoprotein in Ph$^+$ CML blasts (4), as well as a target of v-Abl kinase activity in v-Abl–transformed B

A. Di Cristofano's present address is Human Genetics Program, Fox Chase Cancer Center, Philadelphia, PA 19111.

Address correspondence to Pier Paolo Pandolfi, Department of Human Genetics, Box 110 Memorial Sloan-Kettering Cancer Center, 1275 York Ave., New York, NY 10021. Phone: 212-639-6168; Fax: 212-717-3102; E-mail: p-pandolfi@ski.mskcc.org

**Abbreviations used in this paper:* BMMC, bone marrow–derived mast cell; CML, chronic myelogenous leukemia; EGF, epidermal growth factor; ES, embryonic stem; KL, kit ligand; MAPK, mitogen-activated protein kinase; PDGF, platelet-derived growth factor; PEF, primary embryonic fibroblast.

cells (5). It contains a pleckstrin homology (PH) domain in the N-terminal region, followed by a phosphotyrosine binding (PTB) domain also called DKH (Dok homology region, see below), as well as 15 tyrosines and 10 PXXP motifs, most of which are at the COOH-terminal of the protein. Characterization of p62^{dok} revealed its identity to the long-sought RasGAP-associated 62-kD protein which was observed being rapidly phosphorylated in various cells upon activation of many receptors, such as platelet-derived growth factor receptor (PDGFR) (6), epidermal growth factor receptor (EGFR) (7), insulin receptor (8), CSF-1R (9), kit (10), IL-3R and IL-4R (11), B cell receptor (12), FcγRIIB receptor (13), and CD28 (14), and nonreceptor, cytoplasmic kinases such as Tec (15). Furthermore, the phosphorylation status of p62^{dok} was found to be constitutively elevated in v-Src–, v-Fms–, and v-Fps–transformed cells (7, 16). Once phosphorylated, p62^{dok} interacts, through its Src homology 2 (SH2)-binding sites, with a number of signaling molecules such as RasGAP (7), Nck (17), and Csk (13), thus likely placing itself at the crossroads of several signal transduction pathways. The association with RasGAP is particularly intriguing, as p62^{dok} might regulate Ras activity by affecting, for example, the localization and/or the function of GAP.

It has recently become evident that p62^{dok} is a prototype member of a new docking protein family characterized by the presence of a PH domain, a DKH region, and several tyrosine sites and PXXP motifs (18). The additional members of this "dok" (downstream of tyrosine kinases) family include p56^{dok-2} (18) (also called IL-4R interacting protein [FRIP; reference 11] or Dok-R [19]), and dok-3 or DOKL (18, 20, 21). Notably, p56^{dok-2} shares most structural features and the same pattern of expression with p62^{dok}, with the exception of B cells, where p56^{dok-2} is not expressed, thus raising the possibility that these two dok members might exert similar functions.

Given that p62^{dok} can be phosphorylated upon activation of various kinases, it is likely to play an important role in multiple signaling events. Yet, the exact function of p62^{dok} in these events remains unclear. Recently, it has been reported that, in B cells, p62^{dok} negatively regulates mitogen-activated protein kinase (MAPK) activation and cell proliferation upon coaggregation of B cell receptor and FcγRIIB (22, 23). However, it remains to be shown whether p62^{dok} serves a similar role in other cell types and/or upon activation of different receptors or kinases. In fact, studies by Kashige et al. showed that binding of p62^{dok}, phosphorylated by p210$^{bcr-abl}$, to RasGAP resulted in Ras activation in an in vitro biochemistry assay (24), and they suggested that the p210$^{bcr-abl}$ might lead to the activation of Ras through p62^{dok} phosphorylation. To address the above issue, as well as to analyze the biological function of p62^{dok} in a broader context and to determine its relevance as a p210$^{bcr-abl}$ substrate in CML pathogenesis, we have inactivated *p62^{dok}* by homologous recombination. Comparing cells derived from *p62$^{dok-/-}$* and wild-type mice, we show that p62^{dok} is a negative regulator of growth factor–induced cell proliferation in several cell types including mast cells, thymocytes, bone marrow cells, as well as nonhemopoietic primary mouse embryo fibroblasts. We also found that *p62^{dok}* inactivation resulted in sustained activation of Ras and MAPK in primary mast cells and primary embryonic fibroblasts (PEFs) after the removal of growth factor. Nonetheless, the loss of p62^{dok} did not affect DNA damage or growth factor deprivation–induced apoptosis. Furthermore, the transforming ability of p210$^{bcr-abl}$ is not impaired in *p62$^{dok-/-}$* bone marrow cells and, on the contrary, p210$^{bcr-abl}$ causes a fatal myeloproliferative disease with shorter latency in the absence of p62^{dok}. These findings support the notion that dok family members act as negative regulators of cell proliferation and oncogenesis.

Materials and Methods

Generation and Identification of Mutant Mice. A 129/Sv mouse genomic library (Stratagene) was screened with a human *p62^{dok}* cDNA probe. Exon/intron boundaries were determined by restriction enzyme mapping, DNA sequencing, and PCR. To generate the targeting construct, a 2.7-kb HindIII fragment containing 5′ *p62^{dok}* genomic DNA and a 6.9-kb EcoRI-HindII fragment containing 3′ sequence were cloned into pPNT (25). The targeting construct was linearized with NotI and electroporated into CJ7 embryonic stem (ES) cells. Transfectants were selected in G418 (350 μg/ml) and ganciclovir (2 μM) and expanded for Southern blot analysis using 5′ and 3′ external probes (see Fig. 1, A–C). Five correctly recombined clones were obtained screening a total of 120 clones. Chimeric mice were generated by microinjection of two independently generated, targeted ES cell clones with normal karyotypes into E3.5 C57BL6/J blastocysts then transferred to pseudopregnant foster mothers. Chimeric males were mated with C57BL6/J females (The Jackson Laboratory) and germ-line transmission of the mutated allele was verified by Southern blot of tail DNA from agouti coat colored F1 offspring. Chimeras were then mated to 129/Sv females to obtain *p62^{dok}* mutants in the 129/Sv pure background.

Antibodies for Western Blot. Anti-p62^{dok} monoclonal antibody (A-3) was purchased from Santa Cruz Biotechnology, Inc. Anti-actin monoclonal antibody (AC-40) was purchased from Sigma-Aldrich. Phospho-specific antibodies against p44/p42 MAPK (Thr202/Tyr204) and anti-p44/p42 MAPK antibody were from New England Biolabs, Inc.

Preparation of Bone Marrow–derived Mast Cells and In Vitro Cultures. Primary cultures of IL-3–dependent bone marrow–derived mast cells (BMMCs) were prepared from 6-wk-old wild-type or *p62$^{dok-/-}$* mice and maintained as described previously with minor modifications (26). In brief, the mice were killed and the bone marrow was flushed aseptically from femurs and tibias into RPMI 1640 containing 10% heat-inactivated FCS, 50 μM β-mercaptoethanol, 2 mM L-glutamine, 0.1 mM nonessential amino acids, antibiotics (RPMI complete), and 2.5 ng/ml recombinant murine IL-3 (PeproTech). The nonadherent bone marrow cells were maintained at 37°C. Cells were fed with fresh medium every 4 d. After 4 wk of culture, >98% of the cells obtained are BMMCs, as demonstrated by morphological and flow cytometric analysis. For in vitro proliferation assays, BMMCs in RPMI complete medium were starved of IL-3 for 12 h; 10^5 cells were seeded, in triplicate, in 96-well plates, and stimulated with kit ligand (KL) or IL-3 for 24 h. After 20 h, 1 μCi/well of [^{3}H]thymidine was added for 4 h. Cells were harvested and [^{3}H] radioactivity was measured.

Apoptosis Assays. 8×10^6 BMMCs were seeded in 4 ml RPMI with 5% FCS without IL-3 or with 2.5 ng/ml IL-3. Cells were harvested after 24, 48, 72 h of incubation at 37°C, stained with annexin V as per manufacturers' protocol, and the percentage of apoptotic cells was determined by FACS® analysis. For in vivo assays, 6–8-wk-old wild-type and $p62^{dok-/-}$ mice were gamma irradiated with a 10 Gy dose and killed after 6 h. The percentage of apoptotic cells in the thymus and bone marrow was determined by FACS® analysis as described above.

Primary Thymocytes and Mouse Embryo Fibroblast Proliferation Assays. Thymuses from 5–8-wk-old mice were mechanically dissociated by passing through nylon meshes. Contaminating erythrocytes were removed by hypotonic lysis. 2×10^5 cells were cultured in 96-well plates in 100 μl of RPMI 1640 supplemented with 2 mM glutamine, 50 μM β-mercaptoethanol, antibiotics, and 10% FCS. Cells were stimulated by the addition of different concentrations of ConA (Sigma-Aldrich) and/or recombinant mouse IL-2 (Boehringer). For stimulation with plate-bound anti-CD3ϵ antibody (BD PharMingen), plates were coated overnight at 4°C with 10 μg/ml of antibody in PBS, then washed twice with PBS/1% BSA. After 32 h, 1 μCi/well of [^{3}H]thymidine (Amersham Pharmacia Biotech) was added and the cells were harvested 16 h later for [^{3}H]thymidine incorporation determination. Mouse embryo fibroblasts (MEFs) were harvested from 13.5-d-old embryos and cultured in DMEM supplemented with 2 mM glutamine, 50 μM β-mercaptoethanol, antibiotics, and 10% FCS. For proliferation analysis, cells were plated (5×10^4/well) in 96-well plates, serum starved in 0.5% FCS for 24 h, and then stimulated by the addition of 50 ng/ml PDGF (Sigma-Aldrich). After 12 h, 1 μCi/well of [^{3}H]thymidine was added and the cells were harvested 3 h later for [^{3}H]thymidine incorporation.

In Vitro Bone Marrow Cultures. For liquid cultures, bone marrow from 8–16-wk-old mice was obtained by flushing the femurs with IMDM. Contaminating erythrocytes were removed by hypotonic lysis. Live cells were counted and plated (10^6/ml) in RPMI 1640 supplemented with 2 mM glutamine, 50 μM β-mercaptoethanol, antibiotics, 200 μg/ml transferrin (Sigma-Aldrich), 10 μg/ml insulin (Boehringer), 1% BSA, and 10 ng/ml IL-3 (R&D Systems). Live cells were counted at the indicated timepoints by trypan blue exclusion. For cultures in methylcellulose, bone marrow cells were plated in MethoCult GF M3434 (StemCell Technologies Inc.).

MAPK Analysis. PEFs were serum starved in 0.5% FCS for 24 h, and then stimulated for 10 min with 50 ng/ml PDGF, 100 ng/ml EGF (Sigma-Aldrich), or 10 μg/ml insulin (Boehringer). BMMCs were serum starved in RPMI plus 1% FCS for 6 h, and then stimulated for 5 min with 2.5 ng/ml IL-3. At the end of the stimulation, cells were immediately washed with PBS and replated in serum-free medium. At different time points, the cells were washed with ice-cold PBS containing 1 mM sodium vanadate (Na_3VO_4), and lysed in 1 ml ice-cold lysis buffer consisting of 1% Triton X-100, 0.5% NP-40, 150 mM NaCl, 10 mM Tris HCl, pH 7.4, 1 mM EDTA, 1 mM EGTA, 1 mM Na_3VO_4, 10 mM NaF, 1 mM β-glycerophosphate, 25 mM sodium pyrophosphate, and protease inhibitor cocktail (Roche). Cell debris was pelleted, and supernatants containing the whole cell lysates were analyzed on SDS-polyacrylamide gels. Proteins were transferred to nitrocellulose membranes and immunoblotted with phospho-specific p44/p42 MAPK antibody to reveal the presence of activated MAPK. To verify equivalent loading and to confirm the identity of the phosphorylated MAPK, membranes were stripped with 100 mM β-mercaptoethanol, 2% SDS, 62.5 mM Tris (pH 6.7) at 55°C for 30 min and blotted with p44/p42 MAPK antibody. Immunoblots were visualized with enhanced chemiluminescence detection reagents (ECL; Amersham Pharmacia Biotech).

Ras GTP/GDP Binding Analysis. Wild-type and $p62^{dok-/-}$ PEF cells were labeled for 18 h with [^{32}P] Pi (Amersham Pharmacia Biotech) at 0.25 mCi/ml in phosphate-free and serum-free DMEM (Gibco-BRL). The cells were treated with PDGF at 50 ng/ml for 10 min, then twice washed with phosphate-free and serum-free medium and incubated in the same medium for an additional 15 and 30 min. After treatment, the cells were washed twice with ice-cold PBS and lysed in lysis buffer (50 mM Tris-HCl, pH 7.5, 20 mM $MgCl_2$, 150 mM NaCl, 0.5% NP-40, 10 μg/ml aprotinin, 1 mM PMSF) including 4 μg/ml anti–v-H-ras monoclonal antibody (Y13-259; Oncogene Research Products). The cells were scraped off, and harvested by centrifugation. To the supernatants of each sample, 0.1 ml 10% activated charcoal was added. The mixtures were incubated for 1 h and the charcoal was removed by centrifugation. 2 μl of each sample was taken to measure the counts of the samples. Equal counts were taken for each sample and they were then adjusted to the same volume by adding lysis buffer and incubated with 60 μl protein A-Sepharose CL-4B (Amersham Pharmacia Biotech) precoupled with rabbit anti–rat IgG (ICN Biomedicals) for 1.5 h. The beads were precipitated by centrifugation, washed twice with lysis buffer and once with ice-cold PBS, and the nucleotides were eluted with 75 mM KH_2PO_4, pH 3.4, 5 mM EDTA, 2 mM DTT, 0.5 mM GTP, and 0.5 mM GDP at 85°C for 3 min. Separation of eluted nucleotides was on a polyethyleneimine cellulose plate in 0.65 M KH_2PO_4 (pH 3.4). The amount of radioactivity present in the GDP and GTP was quantitated with a PhosphorImager (BAS 2000; Fuji Photo Film Co.). The results represented are an average from three independent experiments.

Bone Marrow Infection and Transplantation Experiments. Transfection of the retroviral construct Mig210, bone marrow isolation from 12-wk-old wild-type and $p62^{dok-/-}$ mice (in the 129/Sv pure genetic background), prestimulation and infection, and transplantation into lethally irradiated 129/Sv mice were performed essentially as follows (see also reference 27): wild-type and $p62^{dok-/-}$ mice were injected with 5 mg of 5-fluorouracil (5-FU). 4 d later, mice were killed, bone marrow cells isolated and subjected to prestimulation in DMEM with 15% FCS, 5% WEHI-3 conditioned medium, 6 ng/ml rmIL-3, 10 ng/ml rmIL-6, and 100 ng/ml rmSCF for 24 h. IL-3, IL-6, and SCF were purchased from PeproTech. After prestimulation, bone marrow cells were infected with the retroviral supernatant in DMEM with 15% FCS, 5% WEHI-3 conditioned medium, 6 ng/ml IL-3, 10 ng/ml IL-6, 100 ng/ml SCF, and 2 μg/ml Polybrene by spin infection using Sorvall RT6000D with 1,000 *g* for 90 min at 37°C. To determine whether inactivation of $p62^{dok}$ affects response to 5-FU and/or prestimulation, bone marrow cells were analyzed before and after prestimulation: (a) by FACS® analysis using combinations of anti–c-kit-PE, anti–CD34-FITC and anti–Mac-1-PE, anti–Gr-1-FITC antibodies; (b) by performing in vitro colony assay in MethoCult GF M3434 (StemCell Technologies Inc.). Colony number was counted on day 7 and 12. No differences were found between the two genotypes. After spin infection and 24 h culture in CO_2 incubator, cells were counted and washed twice in PBS. 5×10^5 cells were injected into the tail vein of irradiated (9.5 Gy as single dose) 129/Sv recipient mice. Infected bone marrow cells were in parallel subjected to FACS® analysis to measure GFP expression and in turn levels of infection by the retrovirus. GFP expression levels in wild-type and $p62^{dok-/-}$ mice derived bone marrow cells were indistinguishable, thus demonstrating that $p62^{dok}$ inactivation does not affect retroviral infection effi-

ciency. Upon transplantation, total and differential counts were performed on peripheral blood cells of recipient mice every 5 d. Cells obtained from peripheral blood and bone marrow of diseased leukemic animals were also analyzed for expression of GFP and Gr-1 markers. Antibodies for FACS® analysis were purchased from BD PharMingen.

Results

Generation of $p62^{dok-/-}$ Mice. To create a $p62^{dok}$ null allele via homologous recombination in mouse ES cells, we isolated genomic clones of the murine $p62^{dok}$ locus screening an isogenic 129/Sv mouse genomic library with a human $p62^{dok}$ cDNA probe. Two overlapping clones were obtained which spanned the $p62^{dok}$ locus. A positive/negative targeting vector, containing 2.7 kb of 5′ and 6.9 kb of 3′ genomic homology in the PNT vector (25), was designed to replace the coding region from exon 1 to part of exon 5 with the neomycin-resistance gene (Neo) cassette (Fig. 1 A). Five mutant CJ7 ES clones heterozygous for the $p62^{dok}$ mutation were generated as described in Materials and Methods section (Fig. 1 B). Two clones, euploid at the karyological analysis, were expanded for injection of C57BL/6 blastocysts. Both clones gave rise to highly chimeric mice that were then mated with C57BL/6 females to obtain germ line transmission of the mutant alleles. Chimeras from both clones transmitted the mutation to the germ line and were subsequently mated to 129/Sv females to obtain $p62^{dok}$ heterozygotes (+/−) in a pure genetic background. $p62^{dok+/-}$ mice were intercrossed and genotypes were determined by Southern blot (Fig. 1 C). From these crosses, $p62^{dok-/-}$ mice were born following Mendelian frequencies. $p62^{dok-/-}$ mice did not display overt developmental defects and were fertile. Functional disruption of the $p62^{dok}$ gene was confirmed by Western blot analysis of protein extracts from spleen and thymus (Fig. 1 D).

$p62^{dok}$ Controls Cell Proliferation upon Mitogenic Stimuli. Total and differential peripheral blood counts, flow cytometric analysis of peripheral blood, thymus, spleen, and bone marrow, as well as in vitro bone marrow culture under standard conditions (i.e., growth of total marrow in methylcellulose in the presence of hematopoietic growth factors: Materials and Methods) demonstrated that inactivation of $p62^{dok}$ does not affect hematopoiesis in the mouse at the steady state (data not shown).

To determine the effect of $p62^{dok}$ inactivation in the absence of physiological compensatory mechanisms, we analyzed the growth response of wild-type and $p62^{dok-/-}$ hemopoietic and fibroblast cells to mitogenic stimuli. As $p62^{dok}$ is phosphorylated in response to c-kit and IL-3 receptor engagement, we employed BMMCs as a model cell system. BMMCs are a unique model system to study the effects of these cytokines on cell proliferation and apoptosis in a homogeneous population. In fact, although primary totipotent hemopoietic stem cells can not be maintained in long-term cultures, primary BMMCs can be propagated in

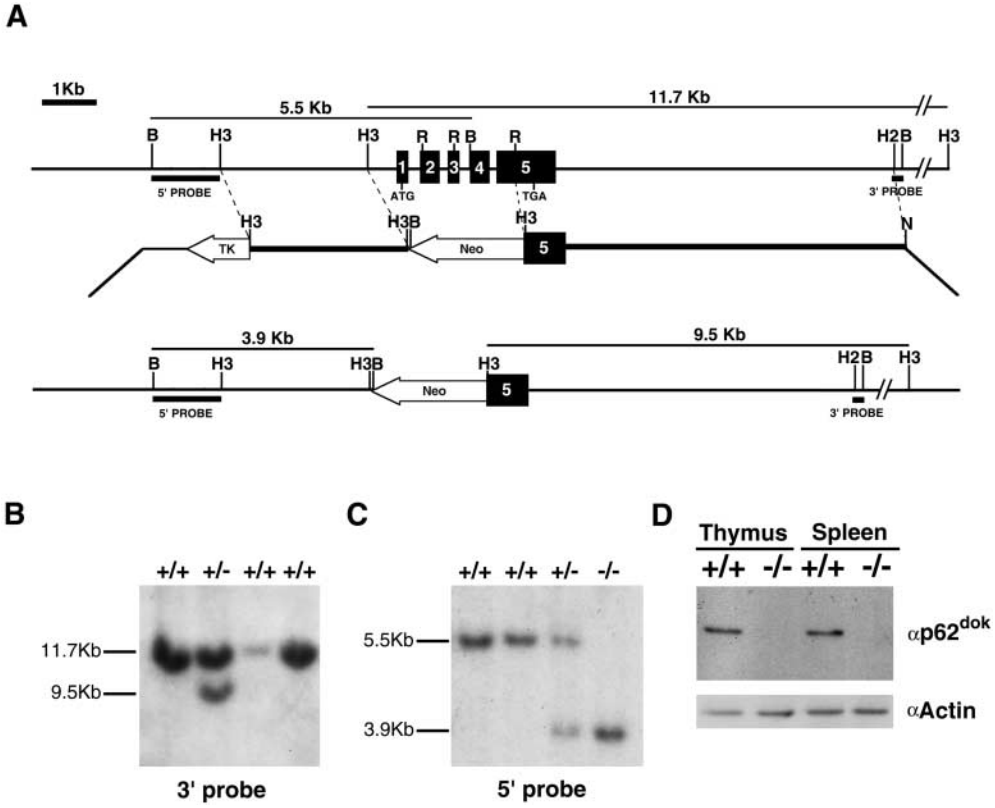

Figure 1. Targeted disruption of the $p62^{dok}$ gene. (A) Structure of the $p62^{dok}$ gene (top), the targeting construct (center), and the predicted structure of the disrupted $p62^{dok}$ gene after homologous recombination (bottom). Only the relevant restriction sites are shown: B, BamH1; H2, HindII; R, EcoR1; H3, HindIII. The numbered solid boxes represent the exons. Neo and TK (herpes simplex virus thymidine kinase) refer to the positive and negative selection markers, respectively. The genomic fragments used as probes for Southern blot analysis are indicated, as well as the expected fragments after hybridization with the two probes, upon digestion with BamH1 and HindIII. (B) Southern blot analysis of ES cells clones after digestion with Hind III and hybridization with the 3′ external probe. (C) Southern blot analysis of BamH1-digested genomic DNA from F2 mice resulting from a cross between two $p62^{dok+/-}$ mice. The blot was hybridized with the 5′ probe. (D) Western blot analysis of thymus and spleen from wild-type and $p62^{dok-/-}$ mice, showing the absence of $p62^{dok}$.

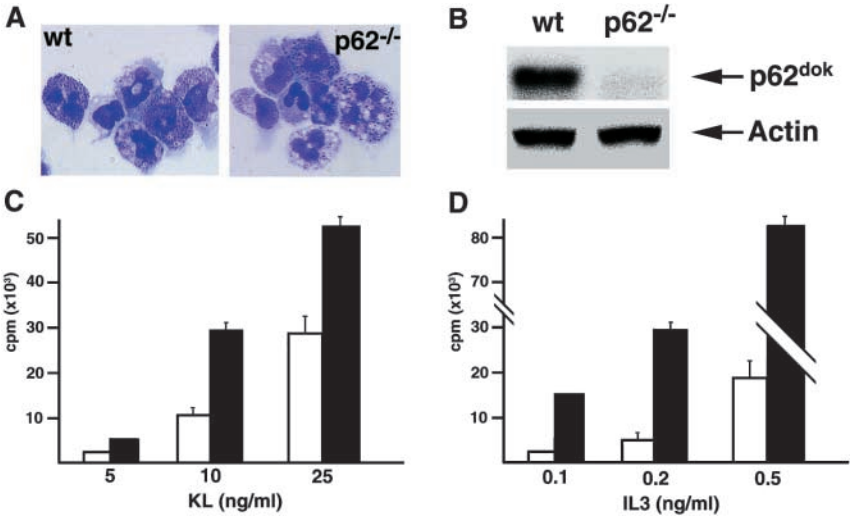

Figure 2. Effect of *p62dok* disruption on BMMCs proliferation. (A) Morphology of wild-type (wt) and $p62^{dok-/-}$ BMMCs. (B) Expression of $p62^{dok}$ and actin detected by Western blot analysis in protein extracts (60 μg) from BMMCs. (C and D) Proliferative response, determined as [^{3}H]thymidine incorporation, of wild-type and $p62^{dok-/-}$ BMMCs upon KL and IL-3 stimulation. Wild-type, white bar; $p62^{dok-/-}$, black bar. All graphs are representative of experiments repeated three to five times. Error bars represent standard deviation.

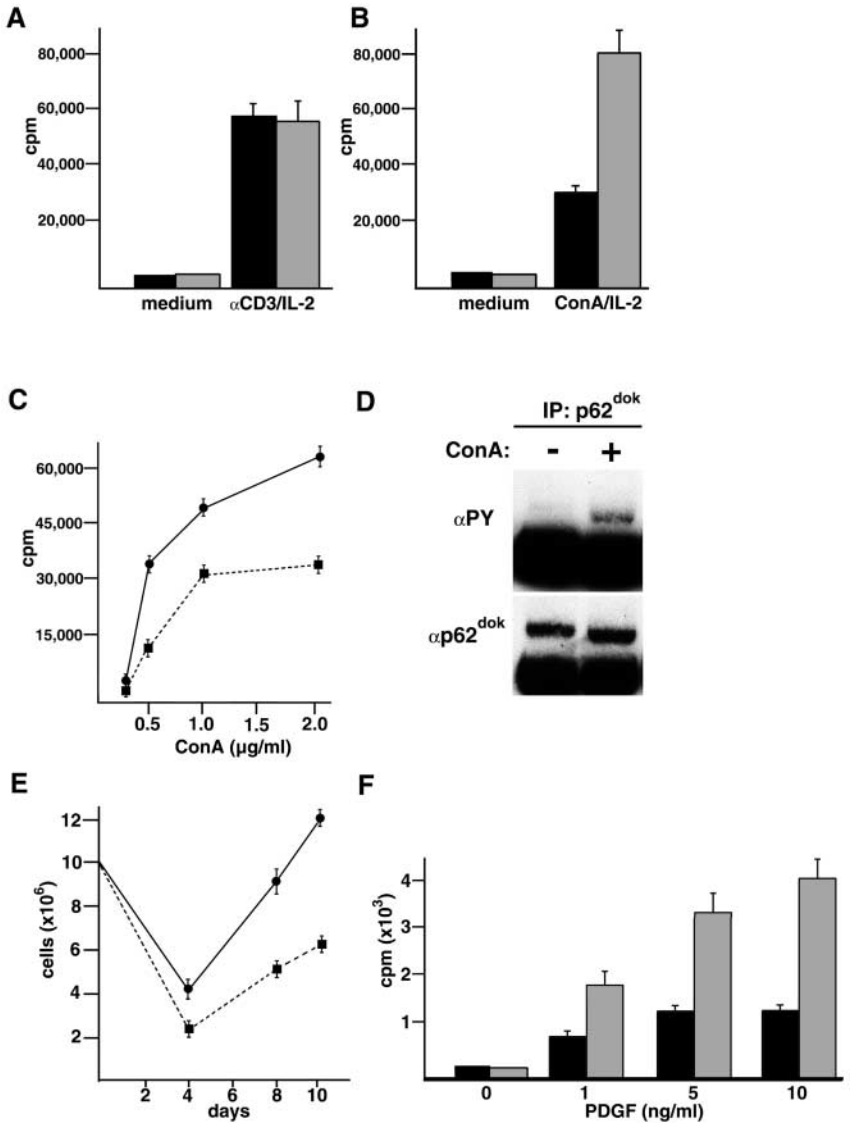

Figure 3. Effect of *p62dok* disruption on cell proliferation in thymocytes, total bone marrow cells and PEFs. (A and B) Proliferative response, determined as [^{3}H]thymidine incorporation, of wild-type and $p62^{dok-/-}$ thymocytes upon plate-bound αCD3ε and ConA (3 μg/ml) stimulation, in the presence of IL-2 (100 U/ml). Wild-type, black bar; $p62^{dok-/-}$, gray bar. (C) Proliferation of wild-type and $p62^{dok-/-}$ thymocytes upon increasing concentrations of ConA and constant amount of IL-2 (100 U/ml). Wild-type, filled square and dashed line; $p62^{dok-/-}$, filled circle and solid line. (D) Phosphorylation of $p62^{dok}$ upon ConA stimulation. (E) In vitro proliferation of wild-type and $p62^{dok-/-}$ bone marrow cells in serum-free medium, in the presence of 10 ng/ml IL-3, measured by manual cell counting. Wild-type, filled square and dashed line; $p62^{dok-/-}$, filled circle and solid line. (F) Proliferative response, determined as [^{3}H]thymidine incorporation, of wild-type and $p62^{dok-/-}$ PEFs upon PDGF stimulation. Wild-type, black bar; $p62^{dok-/-}$, gray bar. All graphs are representative of experiments repeated three to five times. Error bars represent standard deviation.

vitro, express both c-kit and IL-3 receptors, and responses to IL-3 and KL in BMMCs have been well characterized (28, 29). Morphological analysis of wild-type and $p62^{dok-/-}$ BMMCs did not reveal differences between the two cell populations (Fig. 2 A). Moreover, flow cytometric analysis using anti–c-kit, anti–Sca-1, anti–Mac-1, and anti–Gr-1 antibodies showed the same expression levels of these surface molecules (data not shown). Next, we tested by Western blot the expression of $p62^{dok}$ in wild-type and $p62^{dok-/-}$ BMMCs. $p62^{dok}$ protein expression was readily detectable in wild-type BMMCs but not in $p62^{dok-/-}$ cells (Fig. 2 B). The mitogenic effects of KL and IL-3 were characterized by determining the dose-response relationship for KL and IL-3–induced DNA synthesis. Inactivation of $p62^{dok}$ consistently resulted in increased incorporation rates of [^{3}H]thymidine upon treatment of starved BMMCs with low concentrations of these cytokines (Fig. 2, C and D). Thus, $p62^{dok}$ negatively modulates the mitogenic effect of KL and IL-3 in bone marrow mast cells.

To investigate whether the effect of $p62^{dok}$ disruption on mitogenic signals is common to other hemopoietic cell populations, we performed similar assays on thymocytes purified from wild-type and $p62^{dok-/-}$ mice. Thymocytes, maintained in IL-2, were activated with ConA or with plate-bound anti-CD3ε antibody and [^{3}H]thymidine incorporation was subsequently determined. No significant difference was found between wild-type and $p62^{dok-/-}$ thymocytes stimulated with anti-CD3ε (Fig. 3 A), in agreement with the notion that $p62^{dok}$ is not phosphorylated upon CD3 engagement (30). On the contrary, ConA stimulation resulted in a marked increase in [^{3}H]thymidine uptake in the $p62^{dok-/-}$ cells (Fig. 3 B). To ensure that this effect was due to an enhanced sensitivity to ConA, we measured [^{3}H]thymidine incorporation using constant concentration of IL-2 and increasing concentrations of ConA. $p62^{dok-/-}$ cells were hyperresponsive to ConA stimulation in a dose-dependent manner (Fig. 3 C). In contrast, keeping the ConA concentration constant, wild-type and $p62^{dok-/-}$ cells responded to IL-2 in a comparable manner (data not shown). To further assess the involvement of $p62^{dok}$ in the effect triggered by ConA, we compared the phosphorylation status of $p62^{dok}$ in freshly isolated thymocytes and in cells stimulated with ConA for 24 h. As shown in Fig. 3 D, culture of the cells in the presence of ConA resulted in the phosphorylation of $p62^{dok}$. Thus, in thymocytes, ConA induces $p62^{dok}$ phosphorylation, which in turn negatively regulates ConA-induced proliferation.

We next analyzed the response of primary bone marrow cells derived from wild-type and $p62^{dok-/-}$ mice to IL-3, which is a known hemopoietic growth factor. Freshly isolated bone marrow cells were cultured in serum-free medium in the presence of IL-3. $p62^{dok-/-}$ cells showed an increased expansion in response to IL-3 (Fig. 3 E).

To determine whether the aberrant proliferative response observed in $p62^{dok-/-}$ thymocytes and bone marrow cells is shared by nonhemopoietic cell types, we examined the growth properties of wild-type and $p62^{dok-/-}$ PEFs in response to PDGF. Upon PDGF stimulation, $p62^{dok-/-}$ PEFs showed increased levels of [^{3}H]thymidine incorporation compared with wild-type cells (Fig. 3 F). Similar data were obtained for insulin and EGF (data not shown). Thus, $p62^{dok}$ negatively regulates proliferative response to mitogenic stimuli in cells from various histological origins.

$p62^{dok}$ Inactivation Does Not Affect Growth Factor Deprivation and DNA Damage–induced Apoptosis. $p210^{bcr-abl}$ protects hemopoietic cells from apoptotic stimuli such as DNA damage and growth factor withdrawal (31, 32). It is therefore conceivable, at least in principle, that the phosphorylation of $p62^{dok}$ by $p210^{bcr-abl}$ might affect the survival signals generated by the oncoprotein. We therefore determined the effect of $p62^{dok}$ loss on growth factor deprivation–induced apoptosis. To this end, actively proliferating BMMCs were deprived of IL-3 and analyzed at different time points by annexin V staining. $p62^{dok-/-}$ BMMCs underwent apoptosis with the same kinetics and extent as their wild-type counterpart (Fig. 4 A). We next irradiated wild-type and $p62^{dok-/-}$ mice ($n = 4$ and 4) with a 10 Gy dose and examined the apoptotic response of thymocytes and bone marrow cells 6 h after irradiation. No differences were detectable between wild-type and $p62^{dok-/-}$ mice (Fig. 4 B). Thus, disruption of $p62^{dok}$ does not affect the apoptotic response to growth factor deprivation and DNA damage in hemopoietic cells.

Sustained Ras and MAPK Activation in $p62^{dok-/-}$ Cells. To define the molecular basis of the increased proliferative response of $p62^{dok-/-}$ cells, we analyzed the kinetics and extent of MAPK activation upon PDGF stimulation of PEFs. Wild-type and $p62^{dok-/-}$ PEFs were serum starved for 24 h and then treated for 10 min with growth factors. Cells were subsequently washed with PBS and serum-free medium was added. Total protein extracts were prepared from unstimulated cells, growth factor–stimulated cells, as well as 15, 30, and 60 min after removal of growth factors

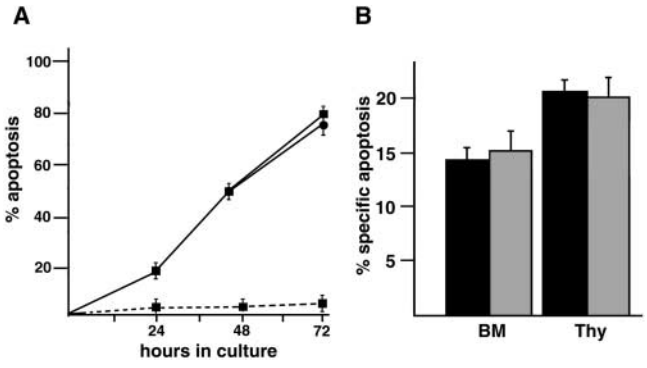

Figure 4. Effect of $p62^{dok}$ disruption on growth factor deprivation and DNA damage–induced apoptosis. (A) Kinetics of the apoptotic response to IL-3 deprivation in BMMCs. Cell death was analyzed by annexin V staining of wild-type (filled square) and $p62^{dok-/-}$ (filled circle) cells at the indicated time points after IL-3 withdrawal (solid lines) or in the presence of IL-3 as a control (dashed lines). (B) In vivo apoptotic response to irradiation. Mice were irradiated (10 Gy) and killed after 6 h. Cell death was analyzed by annexin V staining of bone marrow cells (BM) and thymocytes (Thy). The percent of spontaneous apoptosis in unirradiated littermates has been subtracted from the values shown in the graph. Wild-type, black bar; $p62^{dok-/-}$, gray bar.

to examine the duration of MAPK activation. p62^{dok} was readily phosphorylated in wild-type cells (Fig. 5 A). The analysis of MAPK activation clearly demonstrate that although the level of ERK 1/2 phosphorylation before and during growth factor treatment is comparable in *p62$^{dok-/-}$* and wild-type cells, ERK 1/2 phosphorylation upon growth factor withdrawal is considerably prolonged in *p62$^{dok-/-}$* cells (Fig. 5, A and B). Similar data were obtained using insulin and EGF (data not shown). Rescue experiments in which retroviral-mediated reintroduction of *p62^{dok}* into *p62$^{dok-/-}$* PEFs reversed the increased cell proliferation and the prolonged MAPK activity observed in these cells, proved the specificity of such phenotype (see accompanying paper by Zhao et al.). Therefore, p62^{dok} appears to downregulate the duration of MAPK activity upon growth factor stimulation.

To examine whether the effect of p62^{dok} on MAPK activity occurs through Ras, we labeled the cells and treated them as described above. Cell lysates were subjected to immunoprecipitation with an anti-p21^{ras} antibody. Guanine nucleotides bound to the p21^{ras} immunoprecipitates were separated by TLC and quantified as shown in Fig. 5 C. The basal level of Ras activity was slightly higher in *p62$^{dok-/-}$* when compared with wild-type cells. Furthermore, similar as seen for MAPK activity, the amount of Ras-GTP in *p62$^{dok-/-}$* remained significantly higher after removal of PDGF when compared with wild-type cells, suggesting that p62^{dok} negatively influences Ras signaling.

To determine whether prolonged MAPK activation as a result of *p62^{dok}* inactivation is common to different cell types, and whether this mechanism can be responsible for the increased DNA synthesis rates observed, we analyzed the duration of MAPK activation upon IL-3 stimulation of BMMCs. Once again, removal of IL-3 resulted in a prompt downregulation of MAPK phosphorylation in wild-type cells, whereas the levels of phospho-ERK 1/2 decreased with a slower kinetics in *p62$^{dok-/-}$* cells (Fig. 5, D and E).

p62^{dok} Inactivation Results in Acceleration of Leukemogenesis by p210$^{bcr-abl}$. As p62^{dok} is a major phosphorylation substrate of the p210$^{bcr-abl}$ oncoprotein in CML cells (4), it is

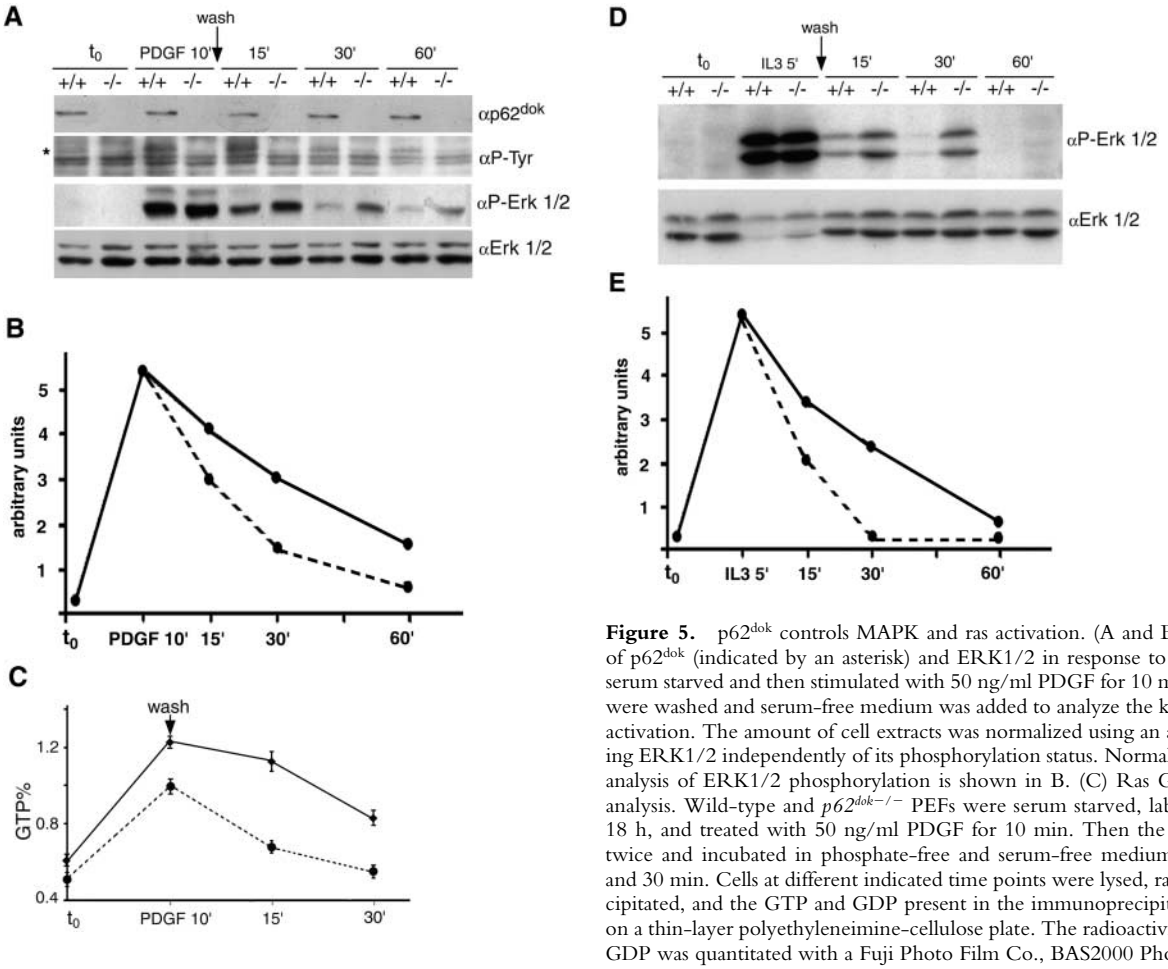

Figure 5. p62^{dok} controls MAPK and ras activation. (A and B) Phosphorylation of p62^{dok} (indicated by an asterisk) and ERK1/2 in response to PDGF. PEF were serum starved and then stimulated with 50 ng/ml PDGF for 10 min. Then, the cells were washed and serum-free medium was added to analyze the kinetics of ERK inactivation. The amount of cell extracts was normalized using an antibody recognizing ERK1/2 independently of its phosphorylation status. Normalized densitometric analysis of ERK1/2 phosphorylation is shown in B. (C) Ras GTP/GDP binding analysis. Wild-type and *p62$^{dok-/-}$* PEFs were serum starved, labeled with ^{32}Pi for 18 h, and treated with 50 ng/ml PDGF for 10 min. Then the cells were washed twice and incubated in phosphate-free and serum-free medium for additional 15 and 30 min. Cells at different indicated time points were lysed, ras was immunoprecipitated, and the GTP and GDP present in the immunoprecipitates were resolved on a thin-layer polyethyleneimine-cellulose plate. The radioactivity in the GTP and GDP was quantitated with a Fuji Photo Film Co., BAS2000 PhosphorImager. The data are expressed as percent GTP, which was calculated by $value_{GTP}$ /(1.5 × $value_{GDP}$ + $value_{GTP}$) × 100. Wild-type, filled circle and dashed line; *p62$^{dok-/-}$*, filled diamond and solid line (D and E). Phosphorylation of ERK1/2 in BMMCs in response to IL-3. BMMCs were serum starved and then stimulated with 2.5 ng/ml IL-3 for 5 min. Then, the cells were washed and serum-free medium was added to analyze the kinetics of ERK inactivation. The amount of cell extracts was normalized using an antibody recognizing ERK1/2 independently of its phosphorylation status. Normalized densitometric analysis of ERK1/2 phosphorylation is shown in E. All graphs are representative examples of experiments repeated three to five times.

possible that it plays an essential role in p210$^{bcr-abl}$–mediated transformation. To address this point, bone marrow cells from wild-type and *p62$^{dok-/-}$* mice in the 129/Sv genetic background were infected with retroviral constructs coexpressing the GFP marker and the p210$^{bcr-abl}$ oncoprotein following a protocol schematically summarized in Fig. 6 A and described in detail in Materials and Methods.

Wild-type and *p62$^{dok-/-}$* transduced cells were transplanted into lethally irradiated 129/Sv mice and total and differential peripheral blood counts were performed every 5 d. Mice transplanted with wild-type–derived bone marrow developed elevated blood counts after day 18 and died between day 21 and day 27 (Fig. 6 B). In mice transplanted with infected bone marrow cells derived from *p62$^{dok-/-}$* mice we observed a marked and significant acceleration of leukemia onset ($P = 0.0018$; Fig. 6 B). In the *p62$^{dok-/-}$* cohort, high blood counts (between 120 and 240 $\times$ $10^3/\mu l$) were observed by day 10, and mice succumbed between day 11 and day 18 (Fig. 6 B). Postmortem pathological analysis in these animals consistently showed in both cohorts hepatosplenomegaly with organs infiltrated by both immature myeloid progenitors and mature granulocytes (not shown). Flow cytometric analysis demonstrated that about 50% of myeloid cells were, as expected, infected with the p210$^{bcr-abl}$ expressing retrovirus (GFP-positive cells) in both genotypes (Fig. 6 C). Flow cytometric and morphological analyses of peripheral blood and bone marrow leukocytes confirmed the myeloid nature of the disease and that the hematological features of the disease in the two groups were indistinguishable (Fig. 6 C, and not shown). Thus, the absence of p62^{dok} does not prevent the ability of p210$^{bcr-abl}$ to transform hemopoietic progenitors, but rather results in the acceleration of the onset of the CML-like disease triggered by p210$^{bcr-abl}$.

Discussion

Phosphorylation of p62^{dok} has been observed after activation of receptor and nonreceptor tyrosine kinases, as well as in relation to oncogenic transformation (6–16). Once phosphorylated, it associates to RasGAP among other signaling molecules, thus leading to the assumption that p62^{dok} might positively regulate cell cycle progression through enhancing Ras signaling pathway. This notion was further corroborated by a recent report, in which in vitro studies showed that binding of p210$^{bcr-abl}$-phosphorylated p62^{dok} to RasGAP resulted in Ras activation (24). However, in vivo studies have showed opposite results and support a model in which p62^{dok} plays a negative role in proliferation induced by coaggregation of B cell receptor and FcγRIIB (22). Our studies confirm and further extend this model, showing that p62^{dok} negatively regulates growth factor–induced cell proliferation, at least in part by negatively regulating Ras and MAPK pathway, as well as p210$^{bcr-abl}$-induced cellular transformation.

p62^{dok} Is a Negative Regulator of Cell Proliferation and Ras and MAPK Activation. We found that, although *p62$^{dok-/-}$* mice are healthy and fertile, null cells of various histological

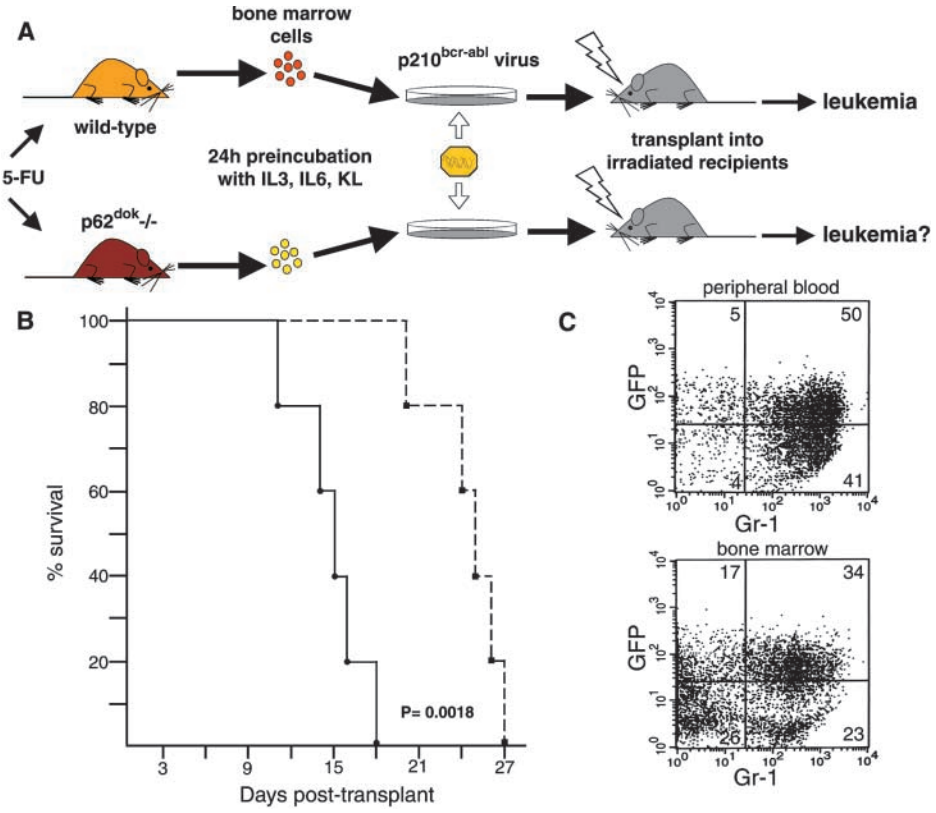

Figure 6. Retroviral transduction of p210$^{bcr-abl}$ results in the transformation of *p62$^{dok-/-}$* bone marrow cells. (A) Schematic representation of the protocol for retroviral transduction of bone marrow and subsequent reconstitution into lethally irradiated recipients (reference 27). (B) Survival of 129/Sv wild-type mice receiving transduced bone marrow cells derived from wild-type (filled square and dashed line) and *p62$^{dok-/-}$* (filled circle and solid line) mice. Log rank statistical analysis was performed to obtain *P*. (C) Flow cytometric analysis of peripheral blood (top), and bone marrow cells (bottom), from a mouse transplanted with p210$^{bcr-abl}$ transduced *p62$^{dok-/-}$* bone marrow cells, using a granulocyte surface marker (Gr-1). In the peripheral blood, almost all the infected cells (cells expressing GFP) coexpress the myeloid-specific marker. In the bone marrow, ~50% of the cells express GFP and >60% of these are Gr-1 positive. A similar immunophenotypical pattern was observed in mice transplanted with wild-type–derived bone marrow (not shown).

origins proliferate faster than wild-type cells in response to growth factor/cytokine stimulation. Furthermore, we observed sustained MAPK activation and prolonged levels of activated (GTP-bound) Ras after growth factor removal. Importantly, our results expand the notion that $p62^{dok}$ is not only a negative regulator of antigen receptor signaling of B cells, but also of signaling events initiated by growth factor receptors in cells of various histological origin including bone marrow cells, which are target of the leukemogenic potential of $p210^{bcr\text{-}abl}$. Furthermore, our data indicate that $p62^{dok}$ may do so, at least in part, by negatively influencing Ras and MAPK activity.

Current studies on other members of the Dok family illustrated consistent results. It was shown that overexpression of $p56^{dok\text{-}2}$ downregulated MAPK activity in response to EGF in Cos-1 cells (33), as well as upon IL-2 stimulation in IL-2Rβ transfected 32D cells (11). Moreover, ectopic expression of dok-3 has been shown to suppress v-Abl–induced MAPK activation and to negatively regulate B cell receptor initiated signaling events, however, independent of MAPK activity (20, 21). Taken together, these observations suggest that the Dok family members negatively influence common as well as distinct physiological signaling events.

Based on the above, it is not so surprising that the inactivation of *$p62^{dok}$* does not lead to an overt phenotype in the mice at the steady state. It is possible that other members of the dok family can compensate for the absence of $p62^{dok}$, especially $p56^{dok\text{-}2}$, which has previously been shown to be very similar to $p62^{dok}$ at the amino acid level and coexpressed with $p62^{dok}$ in most tissues (18). Simultaneous inactivation of two or multiple genes of the Dok family members in the mouse will provide us more insight on their functional characterization.

A Negative Role of $p62^{dok}$ in Leukemogenesis by $p210^{bcr\text{-}abl}$. The identification and characterization of specific targets of $p210^{bcr\text{-}abl}$ aberrant tyrosine kinase activity might uncover the molecular basis underlying the pathogenesis of the chronic phase of CML. Although $p62^{dok}$ was initially thought to be a possible mediator of $p210^{bcr\text{-}abl}$ transforming activity due to its high phosphorylation in CML blasts, its negative role in growth factor signaling events implied that the phosphorylation of $p62^{dok}$ is not required for, even conversely, may oppose the leukemogenic process by $p210^{bcr\text{-}abl}$. Indeed, our results showed that the absence of $p62^{dok}$ did not reduce the ability of $p210^{bcr\text{-}abl}$ to transform the corresponding early hemopoietic progenitors. In fact, mice reconstituted with *$p62^{dok-/-}$* bone marrow cells infected with a $p210^{bcr\text{-}abl}$ retrovirus succumbed with a shorter latency than the controls. Thus, our data indicate that $p62^{dok}$ opposes leukemogenesis by $p210^{bcr\text{-}abl}$. Consistent with the above, Cong et al. showed that overexpression of dok-3 reduced the colony forming ability of v-abl–transformed NIH3T3 cells (20). Moreover, Songyang et al. recently found that overexpression of $p62^{dok}$ diminishes the colony forming ability of v-src–transformed NIH3T3 cells (34).

Given the observed negative regulatory activity of $p62^{dok}$, it is tempting to speculate that $p210^{bcr\text{-}abl}$-triggered phosphorylation of $p62^{dok}$, may lead to the activation of $p62^{dok}$ as a negative regulator, and as such interfering with $p210^{bcr\text{-}abl}$-induced transformation. On the other hand, we can not exclude the possibility that phosphorylation of $p62^{dok}$ triggered by $p210^{bcr\text{-}abl}$ leads to inactivation of $p62^{dok}$'s negative activity in normal signaling events. In the latter case, in cells harboring the $p210^{bcr\text{-}abl}$ oncoprotein, the tumor-growth suppressive activity of $p62^{dok}$ may be partially abrogated. Irrespective of these possibilities, our data conclusively demonstrate that, in vivo, $p62^{dok}$ is not required for the transduction of the leukemogenic signal and that its loss accelerates oncogenesis by $p210^{bcr\text{-}abl}$. Characterization of mice in which two or more Dok genes have been inactivated will provide conclusive evidence in support of the notion that dok proteins can be regarded as bona fide tumor suppressors.

We thank G. Cattoretti, R. Notaro, and C. Cordon-Cardo for help and advice. P.P. Pandolfi is a Scholar of the Leukemia & Lymphoma Society formerly known as the Leukemia Society of America. M. Niki is a fellow of the Charles A. Dana Foundation.

This work is supported by the Sloan-Kettering Institute (through National Institutes of Health grant CA08748) and by the National Institutes of Health (CA64593).

Submitted: 5 March 2001
Revised: 7 May 2001
Accepted: 12 June 2001

References

1. de Klein, A., A.G. van Kessel, G. Grosveld, C.R. Bartram, A. Hagemeijer, D. Bootsma, N.K. Spurr, N. Heisterkamp, J. Groffen, and J.R. Stephenson. 1982. A cellular oncogene is translocated to the Philadelphia chromosome in chronic myelocytic leukaemia. *Nature*. 300:765–767.
2. Lugo, T.G., A.M. Pendergast, A.J. Muller, and O.N. Witte. 1990. Tyrosine kinase activity and transformation potency of bcr-abl oncogene products. *Science*. 247:1079–1082.
3. Clarkson, B., and A. Strife. 1993. Linkage of proliferative and maturational abnormalities in chronic myelogenous leukemia and relevance to treatment. *Leukemia*. 7:1683–1721.
4. Carpino, N., D. Wisniewski, A. Strife, D. Marshak, R. Kobayashi, B. Stillman, and B. Clarkson. 1997. p62(dok): a constitutively tyrosine-phosphorylated, GAP-associated protein in chronic myelogenous leukemia progenitor cells. *Cell*. 88:197–204.
5. Yamanashi, Y., and D. Baltimore. 1997. Identification of the Abl- and rasGAP-associated 62 kDa protein as a docking protein, Dok. *Cell*. 88:205–211.
6. Kaplan, D.R., D.K. Morrison, G. Wong, F. McCormick, and L.T. Williams. 1990. PDGF beta-receptor stimulates tyrosine phosphorylation of GAP and association of GAP with a signaling complex. *Cell*. 61:125–133.
7. Ellis, C., M. Moran, F. McCormick, and T. Pawson. 1990. Phosphorylation of GAP and GAP-associated proteins by transforming and mitogenic tyrosine kinases. *Nature*. 343: 377–381.
8. Hosomi, Y., K. Shii, W. Ogawa, H. Matsuba, M. Yoshida, Y. Okada, K. Yokono, M. Kasuga, S. Baba, and R.A. Roth. 1994. Characterization of a 60-kilodalton substrate of the in-

sulin receptor kinase. *J. Biol. Chem.* 269:11498–11502.
9. Heidaran, M.A., C.J. Molloy, M. Pangelinan, G.G. Choudhury, L.M. Wang, T.P. Fleming, A.Y. Sakaguchi, and J.H. Pierce. 1992. Activation of the colony-stimulating factor 1 receptor leads to the rapid tyrosine phosphorylation of GTPase-activating protein and activation of cellular p21ras. *Oncogene.* 7:147–152.
10. Wisniewski, D., A. Strife, E. Berman, and B. Clarkson. 1996. c-kit ligand stimulates tyrosine phosphorylation of a similar pattern of phosphotyrosyl proteins in primary primitive normal hematopoietic progenitors that are constitutively phosphorylated in comparable primitive progenitors in chronic phase chronic myelogenous leukemia. *Leukemia.* 10:229–237.
11. Nelms, K., A.L. Snow, J. Hu-Li, and W.E. Paul. 1998. FRIP, a hematopoietic cell-specific rasGAP-interacting protein phosphorylated in response to cytokine stimulation. *Immunity.* 9:13–24.
12. Gold, M.R., M.T. Crowley, G.A. Martin, F. McCormick, and A.L. DeFranco. 1993. Targets of B lymphocyte antigen receptor signal transduction include the p21ras GTPase-activating protein (GAP) and two GAP-associated proteins. *J. Immunol.* 150:377–386.
13. Vuica, M., S. Desiderio, and J.P. Schneck. 1997. Differential effects of B cell receptor and B cell receptor-FcgammaRIIB1 engagement on docking of Csk to GTPase-activating protein (GAP)-associated p62. *J. Exp. Med.* 186:259–267.
14. Nunes, J.A., A. Truneh, D. Olive, and D.A. Cantrell. 1996. Signal transduction by CD28 costimulatory receptor on T cells. B7-1 and B7-2 regulation of tyrosine kinase adaptor molecules. *J. Biol. Chem.* 271:1591–1598.
15. Yang, W.C., M. Ghiotto, B. Barbarat, and D. Olive. 1999. The role of Tec protein-tyrosine kinase in T cell signaling. *J. Biol. Chem.* 274:607–617.
16. DeClue, J.E., W.C. Vass, M.R. Johnson, D.W. Stacey, and D.R. Lowy. 1993. Functional role of GTPase-activating protein in cell transformation by pp60v-src. *Mol. Cell. Biol.* 13: 6799–6809.
17. Tang, J., G.S. Feng, and W. Li. 1997. Induced direct binding of the adapter protein Nck to the GTPase-activating protein-associated protein p62 by epidermal growth factor. *Oncogene.* 15:1823–1832.
18. Di Cristofano, A., N. Carpino, N. Dunant, G. Friedland, R. Kobayashi, A. Strife, D. Wisniewski, B. Clarkson, P.P. Pandolfi, and M.D. Resh. 1998. Molecular cloning and characterization of p56dok-2 defines a new family of RasGAP-binding proteins. *J. Biol. Chem.* 273:4827–4830.
19. Jones, N., and D.J. Dumont. 1998. The Tek/Tie2 receptor signals through a novel Dok-related docking protein, Dok-R. *Oncogene.* 17:1097–1108.
20. Cong, F., B. Yuan, and S.P. Goff. 1999. Characterization of a novel member of the DOK family that binds and modulates Abl signaling. *Mol. Cell. Biol.* 19:8314–8325.
21. Lemay, S., D. Davidson, S. Latour, and A. Veillette. 2000. Dok-3, a novel adapter molecule involved in the negative regulation of immunoreceptor signaling. *Mol. Cell. Biol.* 20: 2743–2754.
22. Yamanashi, Y., T. Tamura, T. Kanamori, H. Yamane, H. Nariuchi, T. Yamamoto, and D. Baltimore. 2000. Role of the rasGAP-associated docking protein p62(dok) in negative regulation of B cell receptor-mediated signaling. *Genes Dev.* 14:11–16.
23. Tamir, I., J.C. Stolpa, C.D. Helgason, K. Nakamura, P. Bruhns, M. Daeron, and J.C. Cambier. 2000. The RasGAP-binding protein p62dok is a mediator of inhibitory FcgammaRIIB signals in B cells. *Immunity.* 12:347–358.
24. Kashige, N., N. Carpino, and R. Kobayashi. 2000. Tyrosine phosphorylation of p62dok by p210bcr-abl inhibits RasGAP activity. *Proc. Natl. Acad. Sci. USA.* 97:2093–2098.
25. Tybulewicz, V.L.J., C.E. Crawford, P.K. Jackson, R.T. Bronson, and R.C. Mulligan. 1991. Neonatal lethality and lymphopenia in mice with a homozygous disruption of the *c-abl* proto-oncogene. *Cell.* 65:1153–1163.
26. Timokhina, I., H. Kissel, G. Stella, and P. Besmer. 1998. Kit signaling through PI 3-kinase and Src kinase pathways: an essential role for Rac1 and JNK activation in mast cell proliferation. *EMBO J.* 17:6250–6262.
27. Pear, W.S., J.P. Miller, L. Xu, J.C. Pui, B. Soffer, R.C. Quackenbush, A.M. Pendergast, R. Bronson, J.C. Aster, M.L. Scott, and D. Baltimore. 1998. Efficient and rapid induction of a chronic myelogenous leukemia-like myeloproliferative disease in mice receiving P210 bcr/abl-transduced bone marrow. *Blood.* 92:3780–3792.
28. Chiu, H.F., and B.A. Burrall. 1990. Effect of interleukin 3 on the differentiation and histamine content of cultured bone marrow mast cells. *Agents Actions* 31:197–203.
29. Yee, N.S., I. Paek, and P. Besmer. 1994. Role of kit-ligand in proliferation and suppression of apoptosis in mast cells: basis for radiosensitivity of white spotting and steel mutant mice. *J. Exp. Med.* 179:1777–1787.
30. Klasen, S., F. Pages, J.F. Peyron, D.A. Cantrell, and D. Olive. 1998. Two distinct regions of the CD28 intracytoplasmic domain are involved in the tyrosine phosphorylation of Vav and GTPase activating protein- associated p62 protein. *Int. Immunol.* 10:481–489.
31. Nishii, K., J.H. Kabarowski, D.L. Gibbons, S.D. Griffiths, I. Titley, L.M. Wiedemann, and M.F. Greaves. 1996. ts BCR-ABL kinase activation confers increased resistance to genotoxic damage via cell cycle block. *Oncogene.* 13:2225–2234.
32. Bedi, A., B.A. Zehnbauer, J.P. Barber, S.J. Sharkis, and R.J. Jones. 1994. Inhibition of apoptosis by BCR-ABL in chronic myeloid leukemia. *Blood.* 83:2038–2044.
33. Jones, N., and D.J. Dumont. 1999. Recruitment of dok-R to the EGF receptor through its PTB domain is required for attenuation of erk MAP kinase activation. *Curr. Biol.* 9:1057–1060.
34. Songyang, Z., Y. Yamanashi, D. Liu, and D. Baltimore. 2000. Domain-dependent function of the rasGap binding protein p62Dok in cell signaling. *J. Biol. Chem.* 276:2459–2465.